

# SEM Investigation of the Microstructure of Oxygen-Deficient $\text{Ca}_2\text{FeGaO}_{6-\delta}$

Ariella Fogel, Mandy Guinn, Ram Krishna Hona\*

Environmental Science Department, United Tribes Technical College, Bismarck, USA

Email: \*rhona@utt.edu

**How to cite this paper:** Fogel, A., Guinn, M. and Hona, R.K. (2025) Paper Title. *Journal of Materials Science and Chemical Engineering*, 13, \*-\*.

[https://doi.org/10.4236/jmsce.2025.\\*\\*\\*\\*](https://doi.org/10.4236/jmsce.2025.****)

**Received:** \*\*\*\* \*\*, \*\*\*

**Accepted:** \*\*\*\* \*\*, \*\*\*

**Published:** \*\*\*\* \*\*, \*\*\*

Copyright © 2025 by author(s) and Scientific Research Publishing Inc. This work is licensed under the Creative Commons Attribution International License (CC BY 4.0).

<http://creativecommons.org/licenses/by/4.0/>



Open Access

## Abstract

This study presents a detailed investigation of the microstructure of the oxygen-deficient perovskite material  $\text{Ca}_2\text{FeGaO}_{6-\delta}$  using Scanning Electron Microscopy (SEM). The material exhibits significant porosity and irregular grain morphology, with variations in grain size and growth. Unlike conventional perovskite structures,  $\text{Ca}_2\text{FeGaO}_{6-\delta}$  shows non-uniform grain development, which can be attributed to the presence of oxygen vacancies ( $\delta$ ). SEM analysis reveals that the irregularities in grain size and shape, coupled with the porous nature of the material, are likely to influence its functional properties. These findings provide valuable insights into the structural features of  $\text{Ca}_2\text{FeGaO}_{6-\delta}$  offering a foundation for understanding its potential applications in catalysis, sensors, and other technologies. The study highlights the critical role of microstructural characteristics in determining the material's performance.

## Keywords

XRD, Solid-State Reaction, Perovskite Oxides, Oxygen Deficiency, SEM

## 1. Introduction

Perovskite-related materials, particularly transition metal oxides, have garnered significant attention due to their versatile structural properties and wide range of potential applications in fields such as catalysis, solid oxide fuel cells, electrodes and gas sensors [1]-[4]. Among these materials,  $\text{A}_2\text{BB}'\text{O}_{6-\delta}$ -type double perovskites have shown promise due to their tunable oxygen deficiency, which can enhance their ionic conductivity and catalytic properties [5]. One material of growing interest is  $\text{Ca}_2\text{FeGaO}_{6-\delta}$ , a compound where gallium (Ga) and iron (Fe) occupy the B-sites, forming a unique framework capable of accommodating varying oxygen vacancies ( $\delta$ ) [6].

The characterization of such materials is essential for understanding their structural and electrochemical properties. Scanning Electron Microscopy (SEM) is a powerful technique for investigating the surface morphology and microstructural details at the submicron scale. In the case of  $\text{Ca}_2\text{FeGaO}_{6-\delta}$ , SEM analysis provides critical insights into grain size, texture, and porosity, all of which influence the material's overall performance in technological applications.

This study presents a detailed SEM analysis of  $\text{Ca}_2\text{FeGaO}_{6-\delta}$  focusing on its microstructure and the impact of oxygen vacancies on its morphology. By correlating the SEM data with the material's composition and structural characteristics, we aim to better understand the material's potential for high-performance applications.

## 2. Experimental

Solid-state synthesis method was used to synthesize the material,  $\text{Ca}_2\text{FeGaO}_{6-\delta}$ . The powders of the precursor compounds,  $\text{CaCO}_3$  (Alfa Aesar, 99.95%),  $\text{Fe}_2\text{O}_3$  (Alfa Aesar, 99.998%) and  $\text{Ga}_2\text{O}_3$  (Sigma Aldrich, 99.99%) were mixed in the stoichiometric proportions and ground together using an agate mortar and pestle, pressed into a pellet, and calcined in air at  $1000^\circ\text{C}$  for 24 h in MTI muffle furnace. The samples were then reground and sintered at  $1200^\circ\text{C}$  for 24 h in the same environment, followed by slow cooling. The heating and cooling rates were  $100^\circ\text{C}/\text{h}$ . The phase purity and structure of the polycrystalline samples were determined by powder X-ray diffraction (XRD) at room temperature using  $\text{Cu K}\alpha 1$  radiation ( $\lambda = 1.54056 \text{ \AA}$ ). The GSAS software [7] and EXPGUI interface [8] were used for Rietveld refinements [9]. The microstructures were studied using high-resolution field emission scanning electron microscopy (JEOL-SEM).

## 3. Crystal Structure of $\text{Ca}_2\text{FeGaO}_{6-\delta}$

The oxygen-deficient perovskite  $\text{Ca}_2\text{FeGaO}_{6-\delta}$  crystallizes in the orthorhombic  $Pcmn$  space group [6]. The refined XRD profile of  $\text{Ca}_2\text{FeGaO}_{6-\delta}$  is shown in Figure 1. The structure is derived from the typical  $\text{ABO}_3$  perovskite framework [10], where  $\text{Ca}^{2+}$  ions occupy the A-site, while  $\text{Fe}^{3+}$  and  $\text{Ga}^{3+}$  cations are distributed over the B-site. The oxygen sublattice is incomplete due to the oxygen deficiency, denoted by  $\delta$ , leading to potential oxygen vacancies that affect the material's electrical and ionic conductivity.

In this orthorhombic structure, the  $\text{Fe}^{3+}$  and  $\text{Ga}^{3+}$  cations are octahedrally coordinated by oxygen, forming corner-sharing  $\text{FeO}_6$  and  $\text{GaO}_6$  octahedra. The partial occupancy of oxygen sites due to  $\delta$  introduces distortions in the octahedra, causing deviations from ideal octahedral symmetry. These distortions manifest as tilting and rotation of the octahedra, which are characteristic of oxygen-deficient perovskites and contribute to the overall structural complexity.

The  $\text{Ca}^{2+}$  ions are coordinated by oxygen in an irregular geometry, positioned in the large interstitial sites between the octahedral units. The oxygen vacancies distributed throughout the structure, can significantly influence both the ionic conductivity and the structural stability of the material.

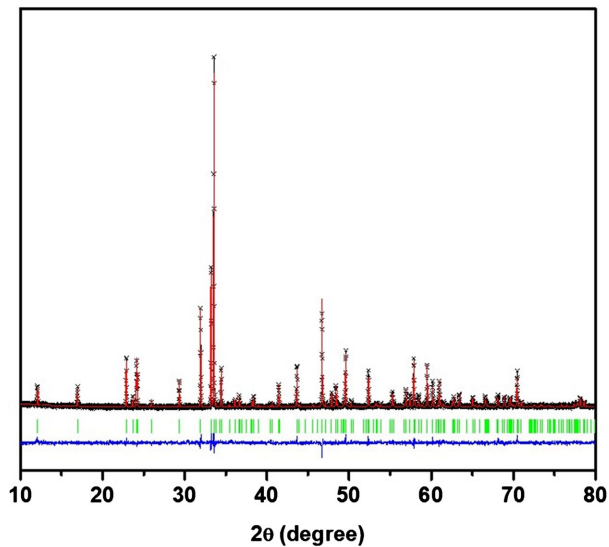


**Figure 1.** Powder X-ray diffraction data of  $\text{Ca}_2\text{FeGaO}_{6-\delta}$ . The black crosses, red lines, green vertical lines, and blue solid lines represent the raw data, the model, Bragg peak positions, and plot differences.

The  $\text{Pc}$  symmetry results in alternating tilts of the  $\text{FeO}_6$  and  $\text{GaO}_6$  octahedra along the  $c$ -axis, while distortions along the  $a$  and  $b$  axes are accommodated through shifts in the positions of the oxygen anions. This tilting system and the oxygen-deficient nature of the material are expected to contribute to unique physical properties, including mixed ionic-electronic conductivity and potential thermoelectric or catalytic behavior.

The unit cell dimensions and atomic coordinates, refined through X-ray diffraction (XRD) studies, reveal that the structure maintains orthorhombic symmetry, though subtle variations in bond lengths and angles arise from the presence of oxygen vacancies and the different ionic radii of  $\text{Fe}^{3+}$  and  $\text{Ga}^{3+}$ . These structural features are key to understanding the material's physical properties, including its electrical conductivity and potential applications in energy-related fields.

#### 4. Scanning Electron Microscopy (SEM) Analysis

The SEM analysis of the oxygen-deficient brownmillerite,  $\text{Ca}_2\text{FeGaO}_{6-\delta}$  reveals crucial insights into the material's surface morphology, particle size distribution, and microstructural characteristics, which are important for understanding its physical and chemical behavior.

The SEM images display a well-defined polycrystalline structure, as shown in **Figure 2**, with grains ranging from sub-micron to a few microns in size. These grains exhibit an irregular shape, often angular or faceted, which is typical of perovskite-derived materials synthesized through solid-state reactions. The grain size ranges from  $6.6 \mu\text{m}$  to  $31.74 \mu\text{m}$  width dimension, as seen in the top left SEM image. The length of the grains ranges from very small to  $33.3 \mu\text{m}$ . The presence of grain boundaries between the crystallites is evident, and these interfaces could play a significant role in ionic and electronic transport within the material.

Additionally, some regions show signs of intergranular porosity, likely a result of oxygen vacancies within the brownmillerite lattice.

At higher magnifications, the microstructure exhibits distinct surface features, such as terrace-like step formations, which are indicative of the layered nature of brownmillerite structures. These terraces arise from the alternating octahedral and tetrahedral layers within the material and contribute to the complex grain morphology. The rough texture observed on the surface may be linked to **oxygen** deficiency ( $\delta$ ), leading to defects and slight lattice distortions that affect surface stability.

Further analysis of the microstructure highlights the presence of micropores and small voids, which are distributed across the grain surfaces. These pores are likely associated with the oxygen vacancy ordering within the brownmillerite phase, contributing to the material's low density and potentially enhancing its catalytic or ion transport properties. The pore distribution may also suggest incomplete densification during the synthesis process, or it could be a result of the loss of oxygen during cooling.

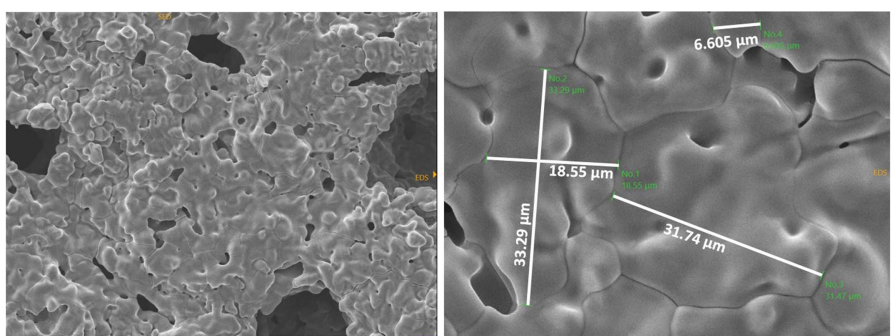


**Figure 2.** SEM images of  $\text{Ca}_2\text{FeGaO}_{6-\delta}$ . Left -  $\times 500$  magnification, and right -  $\times 2000$  magnification.

Energy-dispersive X-ray spectroscopy (EDS) coupled with SEM confirms the elemental composition of the material, showing a uniform distribution of Ca, Fe, Ga, and O across the sample, as displayed in **Figure 3**. The elemental mapping reveals no significant segregation of iron or gallium, suggesting homogeneity within the grains. The oxygen content appears to be slightly reduced in certain regions, further supporting the presence of ordered oxygen vacancies and structural inhomogeneities that contribute to the brownmillerite behavior of  $\text{Ca}_2\text{FeGaO}_{6-\delta}$ .

Porosity decreases a material's thermal **conductivity** or its ability to conduct heat. This is because porosity reduces the number of direct paths for heat conduction, increases thermal resistance, and reduces solid-to-solid contact [11]. The conductivity of a material is determined by how easily electrons can move through it. Collisions between electrons and atoms in the material slow down the electrons and increase the material's resistivity. Materials with higher conductivity allow electrons to move through more easily, resulting in fewer collisions [11].

The overall surface morphology observed in SEM supports the notion that the

microstructural features, including grain size, porosity, and surface roughness, may directly influence the material's electrochemical properties, such as ionic conductivity and catalytic activity. The porosity, in particular, could enhance gas diffusion in catalytic applications, while the grain boundaries may serve as pathways for ionic conduction in energy storage devices.

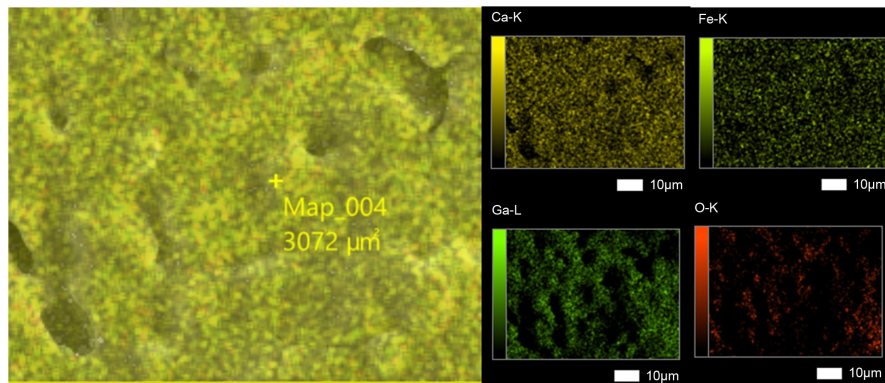


**Figure 3.** SEM images of  $\text{Ca}_2\text{FeGaO}_{6-\delta}$  for elemental mapping.

## 5. Conclusion

In conclusion, the SEM analysis of the oxygen-deficient brownmillerite  $\text{Ca}_2\text{FeGaO}_{6-\delta}$  has provided key insights into the material's microstructural characteristics, including its irregular grain morphology, significant porosity, and the presence of oxygen vacancies. These structural features are strongly linked to the functional properties of the material, particularly its potential in applications requiring catalytic activity, ionic conductivity, and gas diffusion. The non-uniform grain growth and porous structure suggest that oxygen vacancies play a pivotal role in shaping the material's performance, potentially enhancing its reactivity and transport properties. These findings contribute to a deeper understanding of the relationship between the microstructure and the functional behavior of  $\text{Ca}_2\text{FeGaO}_{6-\delta}$  paving the way for further investigations into optimizing its properties for practical applications in energy storage, sensors, and catalytic technologies. Future studies may focus on refining the synthesis process to control grain size and oxygen vacancy distribution, ultimately improving the material's performance in advanced technological applications.

## Acknowledgements

This work is partly supported by the National Science Foundation Tribal College and University Program Instructional Capacity Excellence in TCUP Institutions (ICE-TI) grant award # 2225648. A part of this work is supported by NSF TCUP Tribal Enterprise Advancement Center grant no. HRD 1839895. A part of the work is supported by AIHEC-coordinated NASA TCU Building Bridges, Grant Number 80NSSC24M0025. Additional support for the work came from ND EP-SCOR STEM equipment grants. Permission was granted by the United Tribes

Technical Colleges (UTTC) Environmental Science Department to publish this information. The views expressed are those of the authors and do not necessarily represent those of United Tribes Technical College.

## Conflicts of Interest

The authors declare no conflict of interest.

## References

- [1] Hona, R.K., Karki, S.B. and Ramezanipour, F. (2020) Oxide Electrocatalysts Based on Earth-Abundant Metals for Both Hydrogen- And Oxygen-Evolution Reactions. *ACS Sustainable Chemistry & Engineering*, **8**, 11549-11557.  
<https://doi.org/10.1021/acssuschemeng.0c02498>
- [2] Hona, R.K. and Ramezanipour, F. (2019) Remarkable Oxygen-Evolution Activity of a Perovskite Oxide from the  $\text{Ca}_{2-x}\text{Sr}_x\text{Fe}_2\text{O}_{6-\delta}$  Series. *Angewandte Chemie International Edition*, **58**, 2060-2063. <https://doi.org/10.1002/anie.201813000>
- [3] Hona, R.K., Thapa, A.K. and Ramezanipour, F. (2020) An Anode Material for Lithium-Ion Batteries Based on Oxygen-Deficient Perovskite  $\text{Sr}_2\text{Fe}_2\text{O}_{6-\delta}$ . *Chemistry Select*, **5**, 5706-5711. <https://doi.org/10.1002/slct.202000987>
- [4] Li, Y., Kim, Y.N., Cheng, J., Alonso, J.A., Hu, Z., Chin, Y., *et al.* (2011) Oxygen-Deficient Perovskite  $\text{Sr}_{0.7}\text{Y}_{0.3}\text{CoO}_{2.65-\delta}$  as a Cathode for Intermediate-Temperature Solid Oxide Fuel Cells. *Chemistry of Materials*, **23**, 5037-5044.  
<https://doi.org/10.1021/cm202542q>
- [5] Klyndyuk, A.I., Chizhova, E.A., Kharytonau, D.S. and Medvedev, D.A. (2021) Layered Oxygen-Deficient Double Perovskites as Promising Cathode Materials for Solid Oxide Fuel Cells. *Materials*, **15**, Article 141. <https://doi.org/10.3390/ma15010141>
- [6] Hona, R.K., Huq, A. and Ramezanipour, F. (2019) Charge Transport Properties of  $\text{Ca}_2\text{FeGaO}_{6-\Delta}$  and  $\text{CaSrFeGaO}_{6-\Delta}$ : The Effect of Defect-Order. *Materials Chemistry and Physics*, **238**, Article 121924.  
<https://doi.org/10.1016/j.matchemphys.2019.121924>
- [7] Larson, C.A. and Dreele, R.B.V. (1994) General Structure Analysis System (GSAS). Los Alamos National Laboratory Report LAUR.
- [8] Toby, B.H. (2001) EXPGUI, a Graphical User Interface for GSAS. *Journal of Applied Crystallography*, **34**, 210-213. <https://doi.org/10.1107/s0021889801002242>
- [9] Es-Soufi, H., Bih, H., Bih, L., Rajesh, R., Lima, A.R.F., Sayyed, M.I., *et al.* (2022) Rietveld Refinement, Structural Characterization, and Methylene Blue Adsorption of the New Compound  $\text{Ba}_{0.54}\text{Na}_{0.46}\text{Nb}_{1.29}\text{W}_{0.37}\text{O}_5$ . *Crystals*, **12**, Article 1695.  
<https://doi.org/10.3390/crust12121695>
- [10] Martinson, A., Guinn, M. and Hona, R.K. (2024) The Crystal Structure Study of  $\text{CaSrFe}_{0.75}\text{Co}_{0.75}\text{Mn}_{0.5}\text{O}_{6-\delta}$  by Neutron Diffraction. *Journal of Materials Science and Chemical Engineering*, **12**, 29-35.
- [11] Kultayeva, S., Ha, J., Malik, R., Kim, Y. and Kim, K.J. (2020) Effects of Porosity on Electrical and Thermal Conductivities of Porous Sic Ceramics. *Journal of the European Ceramic Society*, **40**, 996-1004.  
<https://doi.org/10.1016/j.jeurceramsoc.2019.11.045>